Oxygenation in Water

DOI: 10.1002/anie.200801170

Ruthenium-Catalyzed Selective and Efficient Oxygenation of Hydrocarbons with Water as an Oxygen Source**

Yuichirou Hirai, Takahiko Kojima, Yasuhisa Mizutani, Yoshihito Shiota, Kazunari Yoshizawa, and Shunichi Fukuzumi**

The development of methods for the highly selective and efficient conversion of abundant organic resources into valuable products is crucial for a sustainable society. To achieve this goal, extensive studies on the methodology of efficient material conversion with metal complexes as catalysts have been made for a long time.[1,2]

High-valent metal–oxo species are key intermediates in biological oxidations by metalloenzymes (mainly heme and non-heme iron enzymes), which catalyze the oxygenation of hydrocarbons in metabolic and catabolic processes.[3,4] These oxygenases involve high-valent metal–oxo species as reactive species that arise by reductive activation of molecular oxygen coupled with proton transfer.[5–7] Peroxides such as hydrogen peroxide can lead to a so-called "peroxide shunt" to perform the catalytic oxygenation; this mechanism is found for cytochrome P450[8] and methane monooxygenase.[9] Thus, a number of model systems for these enzymatic oxidations have been developed to elucidate the reaction mechanisms and to perform effective catalytic oxygenation of external substrates with metal complexes involving the formation of high-valent metal–oxo species.[10–12] These systems usually require organic solvents and excess amount of organic or inorganic peroxides as both oxidants and oxygen sources. Moreover, in such cases, the reaction pathways become complicated and give multiple products. Consequently it is difficult to control the product distribution that arises mainly from the inevitably produced radical species.[13,14]

Another strategy to generate a high-valent metal–oxo species has been recognized in the oxygen-evolving complex (OEC) in Photosystem II (PS II) for the photosynthesis to oxidize water to produce dioxygen.[15] At the OEC, a manganese(V)–oxo species has been proposed to be formed by proton-coupled electron transfer (PCET), and the deprotonation of coordinated water and the oxidation of the metal center are thought to occur concertedly.[16] This strategy has been applied to form and isolate high-valent metal–oxo species to perform stoichiometric oxidation reactions;[17] however, it has not been applied to catalytic oxidations with transition-metal complexes as catalysts in water.

Inspired by the reactions at the OEC in photosynthesis, we have tried to establish a novel catalytic oxygenation system using water as both the solvent and the oxygen source by virtue of PCET.[18,19] We report herein the formation of a novel ruthenium(IV)–oxo complex and its reactivity toward highly efficient and selective catalytic oxygenation and oxidation reactions of various hydrocarbons in water, which can be used as an oxygen source.

We synthesized a novel bis-aqua Ru^{II} complex, $[Ru^{II}(tpa)(H_2O)_2](PF_6)_2$ (**1**; tpa = tris(2-pyridylmethyl)amine) (Figure 1 a, b), by the treatment of $[Ru^{II}Cl(tpa)]_2(PF_6)_2$[20] with $AgPF_6$ in water. Complex **1** exhibits a reversible two-step deprotonation–protonation equilibrium, and the two pK_a values were determined by UV/Vis spectroscopic titration (see Figure S1 in the Supporting Information) in the range of

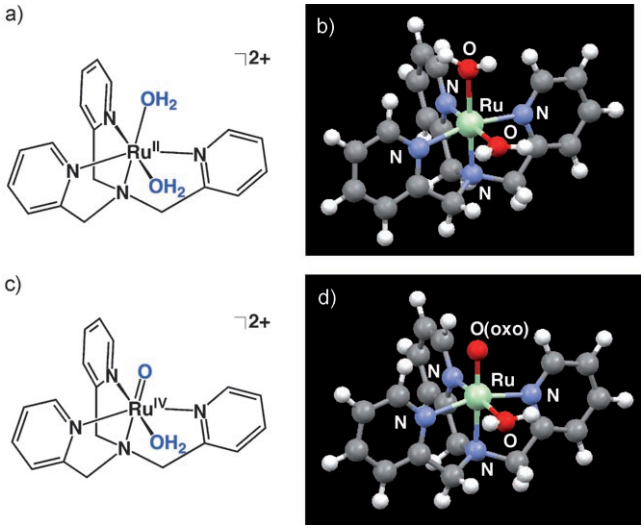

Figure 1. Proposed structures of the cation of complex **1** (a) and that of **2** (c) and their DFT-optimized structures with atom labeling (b for **1** and d for **2**, respectively).

[*] Y. Hirai, Prof. Dr. T. Kojima, Prof. Dr. S. Fukuzumi
Department of Material and Life Science
Graduate School of Engineering
Osaka University and SORST (JST)
2-1 Yamada-oka, Suita, Osaka 565-0871 (Japan)
Fax: (+81) 6-6879-7370
E-mail: kojima@chem.eng.osaka-u.ac.jp
fukuzumi@chem.eng.osaka-u.ac.jp

Prof. Dr. Y. Mizutani
Department of Chemistry
Graduate School of Science, Osaka University
Machikaneyama, Toyonaka, Osaka 560-0043 (Japan)

Dr. Y. Shiota, Prof. Dr. K. Yoshizawa
Institute for Materials Chemistry and Engineering
Kyushu University
Moto-oka, Nishi-Ku, Fukuoka 819-0395 (Japan)

[**] We thank Dr. Yukiyasu Kashiwagi (Osaka National Research Institute) for his accommodation and help to obtain XPS data. This work was supported by a Grant-in-Aid (No. 19205019) from the Ministry of Education, Culture, Sports, Science and Technology, Japan.

Supporting information for this article is available on the WWW under http://dx.doi.org/10.1002/anie.200801170.

© 2008 Wiley-VCH Verlag GmbH & Co. KGaA, Weinheim

$0 < pH < 9$. The first pK_a value is 2.1 for the equilibrium between $[Ru(tpa)(H_2O)_2]^{2+}$ and $[Ru(tpa)(OH)(H_2O)]^+$, and the second value is 8.5 for that between $[Ru(tpa)(OH)(H_2O)]^+$ and $[Ru(tpa)(OH)_2]$. The cyclic voltammogram of **1** measured in the range of $0 < pH < 8$ revealed that complex **1** shows reversible multistep redox behavior in water for oxidation states ranging from Ru^{II} to Ru^{VI}. Each redox couple exhibited a cathodic shift (negative shift) in accordance with the increase of pH (see Figure S2 in the Supporting Information). The Pourbaix diagram of **1** indicates that the redox behavior of **1** is proton-coupled electron transfer; the Ru^{II}/Ru^{III} slope is −62 mV/pH and the Ru^{III}/Ru^{IV} slope is −58 mV/pH in the region of pH 0 to 8 (Figure 2).[21] This result clearly indicates that **1** can give rise to high-valent ruthenium–oxo species by PCET.

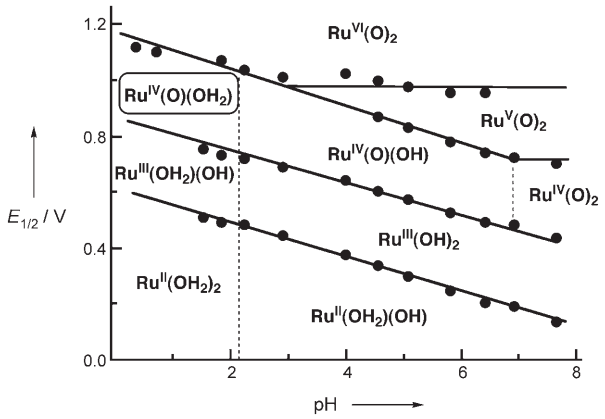

Figure 2. $E_{1/2}$ vs pH plots (Pourbaix diagram) for **1** in aqueous Britton-Robinson buffer. Potentials were determined relative to SCE (as 0 V) at ambient temperature.

The oxidation of **1** (0.9 μmol) with $(NH_4)_2[Ce^{IV}(NO_3)_6]$ (cerium(IV) ammonium nitrate, CAN; 10 μmol) in water (3 mL) resulted in rapid color change from deep green to brown at pH 2.0. The oxidized species exhibits an absorption maximum at 465 nm ($\varepsilon \approx 3 \times 10^3\,M^{-1}\,cm^{-1}$) (Figure 3a). Resonance Raman spectroscopy on the oxidized complex, which was generated by the reaction of **1** (2.5 μmol) with CAN (91 μmol) in $H_2{}^{16}O$ or $H_2{}^{18}O$ (500 μL) at pH 0.5, with excitation at 442 nm allowed us to observe a Raman scattering at 806 cm^{-1} (Figure 3b), assignable to the ruthenium–oxo double bond (Ru=O). When $H_2{}^{18}O$ was employed as a solvent, the peak was observed at 764 cm^{-1} owing to an isotopic shift of $\Delta\nu = 42\,cm^{-1}$. This agrees well with the calculated value for the ^{18}O substitution in a Ru=O harmonic oscillator ($\Delta\nu = 40\,cm^{-1}$) and is crucial evidence for the formation of Ru=O species with water as the oxygen source. In comparison with data for other Ru=O complexes,[22,23] this value falls in the lower region of those due to Ru^{IV}=O, suggesting a rather weak bond. X-ray photoelectron spectroscopy (XPS) was also used to determine the valence of the ruthenium center (see Figure S3 in the Supporting Information). A high-energy shift of the Ru $3d_{3/2}$ peak relative to the peaks of the Ru^{II} or Ru^{III} complexes was observed (286.8 eV), and this value corresponds to that of $Ru^{IV}O_2$.[24,25] These

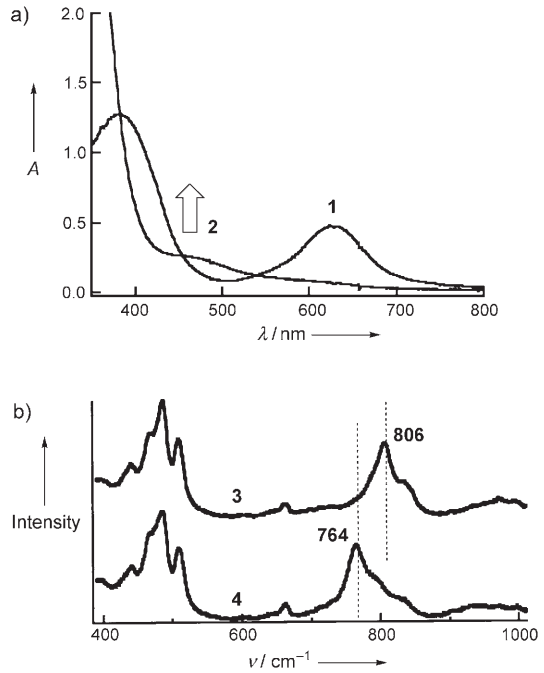

Figure 3. a) UV/Vis spectral change upon addition of CAN (10 μmol) to an aqueous solution of **1** (0.9 μmol) in 3 mL of H_2O at pH 2.0, before (trace 1) and after (trace 2) addition of CAN; b) Resonance Raman spectra of $[Ru^{IV}(^{16}O)(tpa)(H_2O)]^{2+}$ generated in $H_2{}^{16}O$ (trace 3) and $[Ru^{IV}(^{18}O)(tpa)(H_2O)]^{2+}$ generated in $H_2{}^{18}O$ (trace 4); **1** (2.5 μmol) and CAN (91 μmol) in H_2O (500 μL) at pH 0.5; measured at room temperature with 442 nm excitation.

spectroscopic data clearly support the formation of a Ru^{IV}=O complex. Together with the oxidation state obtained from the Pourbaix diagram (Figure 2) (at $pH \approx 0$, $E_{red}(CAN) = 1.0$ V vs SCE in water), we assigned the oxidized complex to be $[Ru^{IV}(O)(tpa)(H_2O)]^{2+}$ (**2**). The Evans' method[26] was applied to determine the spin state of **2** and revealed that **2** has two unpaired electrons, that is, $S = 1$.[27] These unpaired electrons contribute to the radical character of the oxo ligand, which reduces the double-bond character and lowers the ν(Ru=O) energy. Thus, we conclude that the oxidation of **1** by CAN in water affords the intermediate-spin Ru^{IV}=O complex **2**.

We also performed DFT calculations to evaluate the possibility whether the oxo ligand is located at the position *trans* to the tertiary amino group (Figure 1c,d) or *trans* to the axial pyridine moiety (see Figure S4 in the Supporting Information). The former configuration is 6.4 kcal mol^{-1} lower in energy than the latter at the B3LYP/LANL2DZ level of theory.[28] Thus, we assume that the oxo group binds to the position *trans* to the tertiary amino group in **2** as shown in Figure 1c. In the optimized structure, the length of the Ru=O bond is estimated to be 1.804 Å and that of the Ru−OH_2 bond is 2.192 Å. The length of the Ru=O bond falls in the range of those of crystallographically characterized Ru^{IV}=O complexes.[23] The DFT calculations also indicate that the Mulliken spin density is located at the Ru^{IV} center (0.96) and the oxo group (1.05); thus a strong radical character can be expected for the oxo group.

 © 2008 Wiley-VCH Verlag GmbH & Co. KGaA, Weinheim

Catalytic oxidation reactions of organic substrates with CAN (67% purity determined by iodometry) and **1** were examined in water at ambient temperature. When the substrate was insoluble in water, the reaction was carried out in a biphasic system. Product analysis and quantification were made by ^{1}H NMR spectroscopy using [D$_4$]TSP (sodium trimethylsilylpropionate-d_4) as an internal standard.

The catalytic oxygenation of cyclohexene was conducted as follows: A solution containing 0.17 M cyclohexene, CAN, and **1** (molar ratio 100:200:1) in 3 mL of water was stirred at room temperature for 30 min. No reaction occurred in the absence of **1**. ^{1}H NMR and GC-MS analyses of the resultant solution revealed that adipic acid, the product of an 8e oxidation, formed as the sole product, and the catalytic turnover number (TON)[29] was determined to be 25 with 100% oxidant efficiency.[29] The reaction was also conducted in $H_2{}^{18}O$ as the solvent under the same conditions to examine ^{18}O incorporation into the product. In the electron-impact mass spectrum we observed the same fragment pattern as that observed for the authentic adipic acid, with isotopic shifts in the range from 2 to 6. In addition, in the chemical ionization mass spectrum we could observe the molecular ion peak of adipic acid at m/z 155 ($[M+H]^+$); this is 8 units higher than the mass number of the authentic sample. This ensures that all the oxygen atoms derive from water and no radical-chain reactions such as autoxidation were involved even under aerobic conditions.

The scope of further applications of the catalytic system with **1** was also investigated (Table 1). Cyclooctene also affords the corresponding dicarboxylic acid (suberic acid) at slightly elevated temperature (60 °C) (entry 3, Table 1). A water-soluble styrene derivative, sodium styrene-4-sulfonate, is converted to 4-(1,2-dihydroxyethyl)-benzenesulfonate as the acid-catalyzed ring-opened product of the corresponding epoxide, which is the product of 2e oxidation product, in the presence of 2 equiv of CAN (entry 4, Table 1). In the presence of 8 equiv of CAN, the water-soluble styrene derivative can be fully oxidized to give the corresponding benzoic acid and formic acid (entry 5, Table 1) via diol and benzaldehyde intermediates, which can be detected in NMR spectra in the course of the reaction. In sharp contrast, catalytic oxygenation of styrene using 8 equiv of CAN gave benzaldehyde (68%, TON = 68) and benzoic acid (32%, TON = 32) concomitant with formic acid (entry 6, Table 1). An aliphatic terminal olefin, 1-hexene, can be converted to valeric acid and formic acid with 100% selectivity and efficiency (entry 7, Table 1). An aromatic alcohol, benzyl alcohol, can be oxidized to benzaldehyde with 97% selectivity (TON = 84) and with 3% yield of of benzoic acid (TON = 3) (entry 8, Table 1). Aliphatic primary alcohols, 1-propanol (entry 9, Table 1) and 1-butanol (entry 10, Table 1), are oxidized to the corresponding carboxylic acids quantitatively with an efficiency of 100%. More remarkably the C–H oxygenation of saturated hydrocarbon occurs under mild conditions in water: the water-soluble sodium 4-sulfonate-1-ethylbenzene is converted into the corresponding acetophenone derivative selectively (entry 11, Table 1). The alcohol dehydrogenation and ethylbenzene oxygenation should proceed by hydrogen abstraction owing to the radical character of the oxo group, as suggested by the DFT calculations. This catalytic system exhibits high selectivity and the yields of the products mainly depend on the solubility of substrates employed.

For mechanistic insight we focused on the 8e oxidation of cyclohexene to form adipic acid. Cyclohexanediol may be formed from the acid-catalyzed hydrolysis of cyclohexene

Table 1: Catalytic oxidations of various hydrocarbons with the CAN/**1** system in D_2O.[a]

Entry	Substrate	Product (sel. [%])		Conv. [%]	Ox. eff. [%]	TON
1		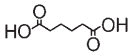	(100)	25	100	25
2[b]		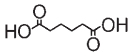	(100)	–[c]	100	2560
3[d]		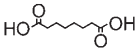	(100)	17	68	17
4	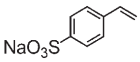	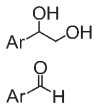	(76) (24)	74	100	56 18
5[e]	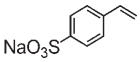	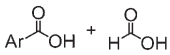	(100)	100	100	100
6[e]		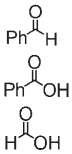	(68) (32) (100)	100	83	68 32 100
7[e]		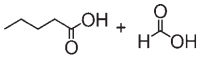	(100)	100	100	100
8			(97)[f]	87	90	84
9			(100)	50	100	50
10			(100)	50	100	50
11	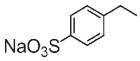		(100)	45	89	45

[a] For procedure and conditions, see the Experimental Section. Ar = 4-benzenesulfonato group. [b] Conducted in 20 mL of D_2O containing cyclohexene (15 mmol) and **1** (0.5 μmol). [c] Not available. [d] Heated to 60 °C and stirred for 4.5 h. [e] CAN (0.8 mmol). [f] Benzoic acid was also formed (3%).

 © 2008 Wiley-VCH Verlag GmbH & Co. KGaA, Weinheim

oxide, and cyclohexanedione may also be formed by two 2e oxidations of the diol. These plausible intermediates en route to adipic acid were submitted to the catalytic conditions to afford adipic acid as the sole product. This supports their involvement as intermediates toward adipic acid. In both cases, the absence of the catalyst **1** afforded a complicated mixture of products, including small amount of adipic acid. This lends credence to the indispensable role of **1** in the selective oxygenation of cyclohexene to form adipic acid. Thus, we propose a reaction mechanism involving the epoxidation of cyclohexene, the hydrolysis of the epoxide to give cyclohexane-1,2-diol, the 4e oxidation of the diol to give cyclohexane-1,2-dione, its subsequent Baeyer–Villiger-like oxidation to give an acid anhydride, and a final hydrolysis under strongly acidic conditions to give adipic acid (Scheme 1).[30] All the oxidation steps are 2e oxidations, which can be performed by **2** as the responsible species.

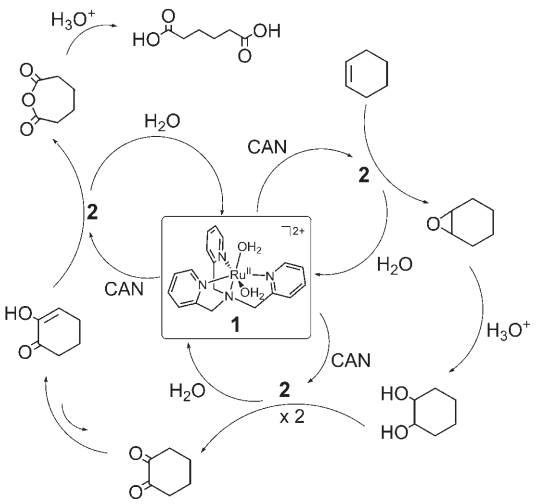

Scheme 1. A proposed mechanism for the catalytic oxygenation of cyclohexene to produce adipic acid in H_2O.

The stepwise mechanism is also supported by the results of the oxidations of the water-soluble styrene derivative given in Table 1 (entries 4 and 5). The amount of CAN added regulates the product distribution; this confirms that the initial product is the diol derived from hydrolysis of the epoxide and that the diol undergoes the C–C bond cleavage to form the aldehyde, which is further converted to benzoic acid and formic acid (see Figure S5 in the Supporting Information).

We evaluated the durability of **1** in the course of the catalysis. An aqueous solution of **1** (5.0×10^{-4} M) was treated with cyclohexene (1.0×10^{-1} M) and CAN (1.2×10^{-2} M), and after the reaction was complete more oxidant was added several times. The production of adipic acid could be duplicated and triplicated with no decrease in the product amount upon addition of further portions of CAN to the same reaction mixture (see Figure S6 in the Supporting Information). The stability of **1** in solution was ensured by UV/Vis and NMR spectroscopy after catalysis was complete. This enables us to establish a persistent catalytic cycle for substrate oxygenation or oxidation. Indeed, we observed a large turnover number of 2560 for adipic acid formation at a lower concentration of **1** and higher concentration of CAN (entry 2, Table 1).

In summary, we have clarified the redox properties of **1** and the formation of the catalytically reactive intermediate-spin Ru^{IV}–oxo species **2** from **1** by PCET. With **1** as a catalyst, we have established a selective and efficient catalytic oxygenation system involving PCET to form reactive species in water, which acts as both the solvent and as the oxygen source. Since catalyst durability has been assured, larger TONs are expected with this system. In addition, according to the Pourbaix diagram we can control the reactive species in accordance with the pH value of the solution. This makes it possible to form $Ru^{V}{=}O$ or $Ru^{VI}(O)_2$ species that probably show higher reactivity than $Ru^{IV}{=}O$ species and allows us access to a wider range of oxidation reactions through the control of pH and the reduction potential of the oxidant.

Experimental Section

Synthesis of $[Ru(tpa)(OH_2)_2](PF_6)_2\cdot(H_2O)$ (**1**$\cdot H_2O$): A mixture including $[RuCl(tpa)]_2(PF_6)_2$ (378.0 mg, 0.33 mmol) and $AgPF_6$ (167.1 mg, 0.66 mmol) in H_2O (33 mL) was refluxed for 12 h. The deep-green solution was filtered through a membrane filter to remove insoluble salt. The filtrate was condensed by rotatory evaporation to give a green precipitate of **1**. The precipitate was filtered and washed with EtOH followed by ether and then dried in vacuo. The yield of isolated **1** was 59% (286 mg). Elemental analysis: calcd for $C_{18}H_{22}N_4O_2RuP_2F_{12}\cdot H_2O$: C 29.32, H 2.96, N 7.72; found: C 29.40, H 3.29, N 7.62.

General procedure for catalytic oxygenation reactions and quantitative method: A solution was prepared in 1 mL of D_2O to contain 0.10 mmol of the substrate and 0.001 mmol of the catalyst **1** and a fixed amount of sodium trimethylsilylpropionate-d_4 ([D_4]TSP) as an internal standard for NMR quantification. The solution was treated with 0.20 mmol of CAN, and the mixture was stirred at room temperature for 30 min. The solution was directly analyzed by ^{1}H NMR spectroscopy. Quantitative analysis was made on the basis of calibration of peak integration of authentic sample relative to TSP.

Received: March 11, 2008
Published online: June 20, 2008

Keywords: cerium · homogeneous catalysis · oxidation · redox chemistry · ruthenium

[1] A. E. Shilov, G. B. Shul'pin, *Chem. Rev.* **1997**, *97*, 2879–2932.
[2] T. Punniyamurthy, S. Velusamy, J. Iqbal, *Chem. Rev.* **2005**, *105*, 2329–2363.
[3] *Cytochrome P450, Structure, Mechanism, and Biochemistry*, 2nd ed. (Ed: P. R. Ortiz de Montellano), Prenum, New York, **1995**.
[4] I. Schlichting, J. Berendzen, K. Chu, A. M. Stock, S. A. Maves, D. E. Benson, R. M. Sweet, D. Ringe, G. A. Petsko, S. G. Sliger, *Science* **2000**, *287*, 1615–1622.
[5] S.-K. Lee, B. G. Fox, W. A. Froland, J. D. Lipscomb, E. Münck, *J. Am. Chem. Soc.* **1993**, *115*, 6450–6451.
[6] G. L. Berglund, G. H. Carlsson, A. T. Smith, H. Szöke, A. Henriksen, J. Hadju, *Nature* **2002**, *417*, 463–468.
[7] B. Meunier, S. P. Visser, S. Shaik, *Chem. Rev.* **2004**, *104*, 3947–3980.

 © 2008 Wiley-VCH Verlag GmbH & Co. KGaA, Weinheim

[8] J. T. Groves, Y.-z. Han in *Cytochrome P450, Structure, Mechanism, and Biochemistry*, 2nd ed. (Ed: P. R. Ortiz de Montellano), Prenum, New York, **1995**, pp. 3–48.
[9] W. A. Froland, K. K. Andersson, S.-K. Lee, Y. Liu, J. D. Lipscomb, *J. Biol. Chem.* **1992**, *267*, 17588–17597.
[10] J. T. Groves, Y. Watanabe, *J. Am. Chem. Soc.* **1988**, *110*, 8443–8452.
[11] L. Que, Jr., *Acc. Chem. Res.* **2007**, *40*, 493–500.
[12] W. Nam, *Acc. Chem. Res.* **2007**, *40*, 522–531.
[13] T. Kojima, K. Hayashi, S. Iizuka, F. Tani, Y. Naruta, M. Kawano, Y. Ohashi, Y. Hirai, K. Ohkubo, Y. Matsuda, S. Fukuzumi, *Chem. Eur. J.* **2007**, *13*, 8212–8222.
[14] R. A. Sheldon, J. K. Kochi, *Metal-Catalyzed Oxidations of Organic Compounds*, Academic Press, New York, **1981**.
[15] J. P. McEvoy, G. W. Brudvig, *Chem. Rev.* **2006**, *106*, 4455–4483.
[16] M. H. V. Huynh, T. J. Meyer, *Chem. Rev.* **2007**, *107*, 5004–5064.
[17] C.-M. Che, V. W.-W. Yam, T. C. W. Mak, *J. Am. Chem. Soc.* **1990**, *112*, 2284–2291.
[18] A. S. Goldstein, R. H. Beer, R. S. Drago, *J. Am. Chem. Soc.* **1994**, *116*, 2424–2429.
[19] a) J. A. Gilbert, D. S. Eggleston, W. R. Murphy, Jr., D. A. Geselowitz, S. W. Gersten, D. J. Hodgson, and T. J. Meyer, *J. Am. Chem. Soc.* **1985**, *107*, 3855–3864; b) T. J. Meyer, M. H. V. Huynh, *Inorg. Chem.* **2003**, *42*, 8140–8160.
[20] T. Kojima, T. Amano, Y. Ishii, M. Ohba, Y. Okaue, Y. Matsuda, *Inorg. Chem.* **1998**, *37*, 4076–4085.
[21] J. C. Dobson, T. J. Meyer, *Inorg. Chem.* **1988**, *27*, 3283–3291.
[22] I. R. Paeng, K. Nakamoto, *J. Am. Chem. Soc.* **1990**, *112*, 3289–3297.
[23] C.-M. Che, T.-F. Lai, K.-Y. Wong, *Inorg. Chem.* **1987**, *26*, 2289–2299.
[24] D. Rochefort, P. Dabo, D. Guay, P. M. A. Sherwood, *Electrochim. Acta* **2003**, *48*, 4245–4252.
[25] K. Kobayashi, H. Ohtsu, T. Wada, T. Kato, K. Tanaka, *J. Am. Chem. Soc.* **2003**, *125*, 6729–6739.
[26] D. F. Evans, D. A. Jakubovic, *J. Chem. Soc. Dalton Trans.* **1988**, 2927–2933.
[27] a) C. M. Che, W.-T. Tang, W.-T. Wong, T.-F. Lai, *J. Am. Chem. Soc.* **1989**, *111*, 9048–9056; b) W.-H. Leung, C. M. Che, *J. Am. Chem. Soc.* **1989**, *111*, 8812–8818; c) for comparison, see Ref. [19b].
[28] DFT calculations were made for $[Ru(O)(tpa)(H_2O)]^{2+}$ under the restriction of the $S=1$ state.
[29] Oxidant efficiency is calculated as [products(mol) per added CAN(mol) $\times$ N(oxidation equivalent)] $\times$ 100. Turnover number (TON) is calculated as [product(mol) per catalyst(mol)].
[30] A similar reaction mechanism was proposed: K. Sato, M. Aoki, R. Noyori, *Science* **1998**, *281*, 1646–1647.

 © 2008 Wiley-VCH Verlag GmbH & Co. KGaA, Weinheim